Quality Improvement Study

Medicine®

OPEN

Branch ostial optimization treatment and optimized provisional t-stenting with polymeric bioresorbable scaffolds

Ex-vivo morphologic and hemodynamic examination

Wei Cai, MD, PhD[a,b], Lianglong Chen, MD, PhD, FESC, FACC[a,b,*], Linlin Zhang, MD, PhD[a,b], Sheng Tu, MD, PhD[a,b], Lin Fan, MD, PhD, FEAPCI[a,b], Zhaoyang Chen, MD, PhD[a,b], Yukun Luo, MD, PhD[a,b], Xingchun Zheng, MD[a,b]

Abstract

The optimal side-branch (SB) ostium treatment after provisional side-branch scaffolding remains a subject of debate in bioresorbable vascular scaffold (BVS) era. In this study, we evaluated a novel optimized provisional T-stenting technique (OPT) and assessed its feasibility by comparison with T and small protrusion technique (TAP).

Two provisional SB scaffolding techniques (OPT, n = 5; TAP, n = 5) were performed using polymeric BVS in a bifurcated phantom. The sequential intermediate snuggling balloon dilation, also called ostial optimal technique, was added to OPT but not TAP to dilate the side-branch ostium while the final snuggling balloon dilation applied for both procedures. Microcomputed tomography (microCT) and optical coherence tomography (OCT) were performed to assess morphology, and computational fluid dynamics (CFD) was performed to assess hemodynamics in the scaffolded bifurcations. Compared with TAP in microCT analysis, OPT created shorter neo-carina length than TAP (0.34 ± 0.10 mm vs 1.02 ± 0.26 mm, $P < .01$), longer valgus struts length (2.49 ± 0.27 mm vs 1.78 ± 0.33 mm, $P < .01$) with larger MB ostial area (9.46 ± 0.04 mm^2 vs 8.34 ± 0.09 mm^2, $P < .01$). OCT found that OPT significantly decreased the struts mal-apposition (13.20 ± 0.16% vs 1.94 ± 0.54%, $P < .01$). CFD revealed that OPT generated more favorable flow pattern than TAP, as indicated by less percent (4.68 ± 1.40% vs 8.88 ± 1.21%, $P < .01$) of low wall shear stress (<0.4 Pa) along the lateral walls.

By using BVSs for bifurcation intervention, the sequential intermediate snuggling balloon dilation is feasible for optimizing ostial SB and facilitating subsequent SB scaffolding. Results show OPT is better than TAP for bifurcated morphology and hemodynamics in this ex-vivo study.

Abbreviations: BCD = bifurcated connecting domain, BVS = bioresorbable vascular scaffold, CFD = computational fluid dynamics, CPT = classic provisional T-stenting, EBC = European bifurcation club, microCT = microcomputed tomography, OCT = optical coherence tomography, OOT = ostial optimization technique, OPT = optimized provisional T-stenting, TAP = T and small protrusion technique.

Keywords: bifurcation, bioresorbable vascular scaffold, coronary artery disease, optical coherence tomography, X-ray microtomography

1. Introduction

Percutaneous coronary intervention (PCI) of coronary bifurcation lesions (CBLs) remains challenging. It is associated with a higher rate of major adverse cardiac events than PCI of non-CBLs (15.2% vs 8.0%, $P = .009$).[1] Bioresorbable vascular scaffolds (BVSs) are novel intracoronary therapeutic devices that can be completely absorbed within 2 to 3 years postprocedure. However, systematic evaluation of BVSs in the treatment of CBLs and more secure and effective technological optimizations are still lacking.

In the era of metal drug-eluting stents, simple strategy (1-stent) was the default for the majority of CBLs as most previous studies had not shown additional benefits of complex strategy (2-stent).[1–5] Similarly, in the era of BVSs, 1-stent or provisional T-stenting is also preferred for PCI of CBLs, as recommended by the European Bifurcation Club (EBC) because current polymeric BVSs may not be suitable for most 2-stent techniques.[6–10]

Classic provisional T-stenting (CPT) offers options of 1-stent or 2-stent technique. However, CPT may be associated with incomplete scaffold coverage so there may be a gap in the upper rim of the ostial side-branch (SB) particularly in Y-type CBLs. Although T and small protrusion technique (TAP) greatly eases the SB stent positioning with complete lesion coverage, stent over-protrusion into the proximal main-vessel (PMV) will alter bifurcated morphologies and hemodynamics, increasing the risk

Editor: Salvatore De Rosa.

This study was supported by the National Natural Science Foundation of China (mainly by Grant No. 81670332, partially by Grant No. 81370311).

The authors have no conflicts of interest to disclose.

Supplemental Digital Content is available for this article.

[a] Department of Cardiology, Fujian Medical University Union Hospital, [b] Provincial Institute of Coronary Artery Disease, Fujian, PR of China.

[*] Correspondence: Lianglong Chen, Xinquan Road 29, Fuzhou, Fujian 350001, PR of China (e-mail: lianglongchenfj@126.com).

Medicine (2018) 97:43(e12972)

Received: 19 May 2018 / Accepted: 1 October 2018

http://dx.doi.org/10.1097/MD.0000000000012972

of thrombosis and restenosis. In the use of BVS, carefully selected patients with simple lesions (e.g., left main lesions, bifurcation lesions with side branch diameters >2 mm diameter, ostial lesions, lesions with moderate, or heavy calcification were excluded) are treated with simple techniques (provisional strategy). It is possible that BVS may increase the incidence of scaffold thrombosis when used in patients with complex diseases, such as bifurcated, defuse, or calcified lesions.[7,9,11,12] Recent studies have shown that polymeric BVS significantly increases scaffold thrombosis by approximately 2 to 3 folds,[13–18] which might be related to the suboptimal implantation technique. Although Abbott has stopped selling Absorb BVS, this is not the end of the bioresorbable platform. Other BRS with different designs (e.g., NeoVas, Firesorb) are now under investigation and have been shown noninferior to CoCr-EES.[19] For this reason, previous stenting techniques should be re-examined in the BVS era, particularly those for the treatment of complex lesion subsets, for instance, CBLs.

Herein, ostial optimization technique (OOT) is proposed as a means of optimizing the SB ostium after stenting the main-branch (MB).[20] In one of our previous studies in which metal stents were used, results suggested that OOT was able to reposition the redundant MB struts over the superior border of the SB ostium (struts ectropion). These results show that 1-stent implantation can have the same effects as 2-stent implantation in rescue SB stenting. OOT can also facilitate subsequent stent positioning and implantation without causing the struts to protrude into the PMV when the single stenting procedure was converted to a bailout T-stenting or TAP procedure. The latter was called provisional T-stenting with OOT or optimized provisional T-stenting (OPT). It is unclear if the BVS performs better when inserted using the OOT or OPT bifurcation techniques. We simulated 2 different provisional T-stenting procedures with or without OOT in vitro to optimize the technical procedure using BVS.

The goals of the present study are to assess the technical feasibility of OOT in optimizing the SB ostium, and to compare the bifurcated scaffold morphologies and hemodynamics of TAP and OPT with respect to polymeric BVS.

2. Methods

2.1. Experiment protocol

A bifurcation model with a distal bifurcation angle of 60°, made of polyvinyl alcohol based on Murray law (proximal main vessel = 0.678 [distal main vessel diameter + side branch diameter]), was adopted for bench testing, which was incubated in a water bath of 37°C.

Two provisional T-stenting techniques (OPT, n = 5; TAP, n = 5) were performed using polymeric BVS (NeoVas, LePu Medical, Beijing, China) to scaffold the MB (3.5 mm BVS) and SB (3.0 mm BVS). A compliance balloon (Apex, Boston Scientific, Maple Grove) was used for pretreating the scaffold side-hole and noncompliance balloon (Quantum Maverick, Boston Scientific, Maple Grove) for postdilation including intermediate/final snuggling balloon dilation and proximal optimization technique (POT). The study was approved by and conformed to the Ethics Committee of Fujian Medical University.

2.2. Scaffolding procedures

The steps in the OPT procedure are as follows (Appendix Figure A, http://links.lww.com/MD/C579):

1. Implanting the PMV-MB scaffold with a slow increase of 2 atmospheres every 5 seconds and up to 10 atmospheres for 30 seconds.
2. POT with a noncompliant balloon at 14 atmospheres to facilitate rewiring of the SB through the most distal cell of the MB scaffold facing the SB ostium.
3. Sequential intermediate snuggling balloon dilation to optimize the ostial SB, which was achieved by first inflating the SB noncompliant balloon at 10 atmospheres and then MB noncompliant balloons at 6 atmospheres for 30 seconds to overturn the redundant struts covering the SB ostium onto the superior border of the ostial SB (OOT).
4. Deploying the rescue scaffold through the open struts into the side branch, and not requiring of strut protrusion into the PMV for complete coverage of the ostial SB as implanting the SB scaffold at 10 atmospheres for 30 seconds.
5. Final snuggling balloon dilation with 2 noncompliance balloons at 8 atmospheres for 30 seconds.
6. Re-POT with a noncompliant balloon at 14 atmospheres for 30 seconds to end the procedure.

The steps in the TAP procedure are as follows (Appendix Figure B, http://links.lww.com/MD/C579): Implanting the PMV-MB scaffold with a slow increase of 2 atmospheres every 5 seconds and up to 10 atmospheres for 30 seconds. POT with a noncompliant balloon at 14 atmospheres to facilitate rewiring of the SB through the most distal cell of the MB scaffold facing the SB ostium. Routine intermediate balloon dilation (non-OOT) by concurrently inflating the SB and MB noncompliant balloons both at 8 atmospheres for 30 seconds to dilate the SB ostium. Implantation of the SB scaffold at 10 atmospheres for 30 seconds with partial strut protrusion into the PMV for complete coverage of ostial SB. Final snuggling balloon dilation with 2 noncompliance balloons at 8 atmospheres for 30 seconds. Re-POT with a noncompliant balloon at 14 atmospheres for 30 seconds to end the procedure.

2.3. MicroCT scanning with raw data acquisition and 3D reconstruction

Each step was observed visually and recorded with a digital recorder (L-1ex/TT02RX, ELMO, Japan) and the final results were acquired by microcomputed tomography (microCT) (Sky-Scan 1176, Kontich, Belgium). The scanning method and settings were: the sample was positioned on a rotary plate with 360° rotation at the speed of 0.36°/s, with a total of 800 to 1000 images recorded per sample. The X-ray parameter was set at 65 kV and 385 μA, and scanning with high spatial resolution of 18 μm. After postprocessing, three-dimensional (3D) reconstruction was performed as previously described.[21]

2.4. Morphological analysis

The bifurcated scaffolds were segmented into 4 parts with PMV, MB, SB, and polygon of confluence (POC) (Fig. 1A), and POC and its adjacent segments (3 mm proximal to POC, 3 mm distal to SB and MB ostium) were defined as the bifurcated connecting domain (BCD) (Fig. 1B). MicroCT was used to measure the length (L_{VS}) and angle (A_{VS}) of valgus struts (Fig. 1B) in the stage of SB ostial treatment (OOT/non-OOT) and to assess following parameters in the stage of SB scaffolding (OPT/TAP): the length of neo-carina (L_{NC}), the area of referent (A_{REF}), and minimal (A_{MIN}) scaffold lumen in each segment, the area of the MB

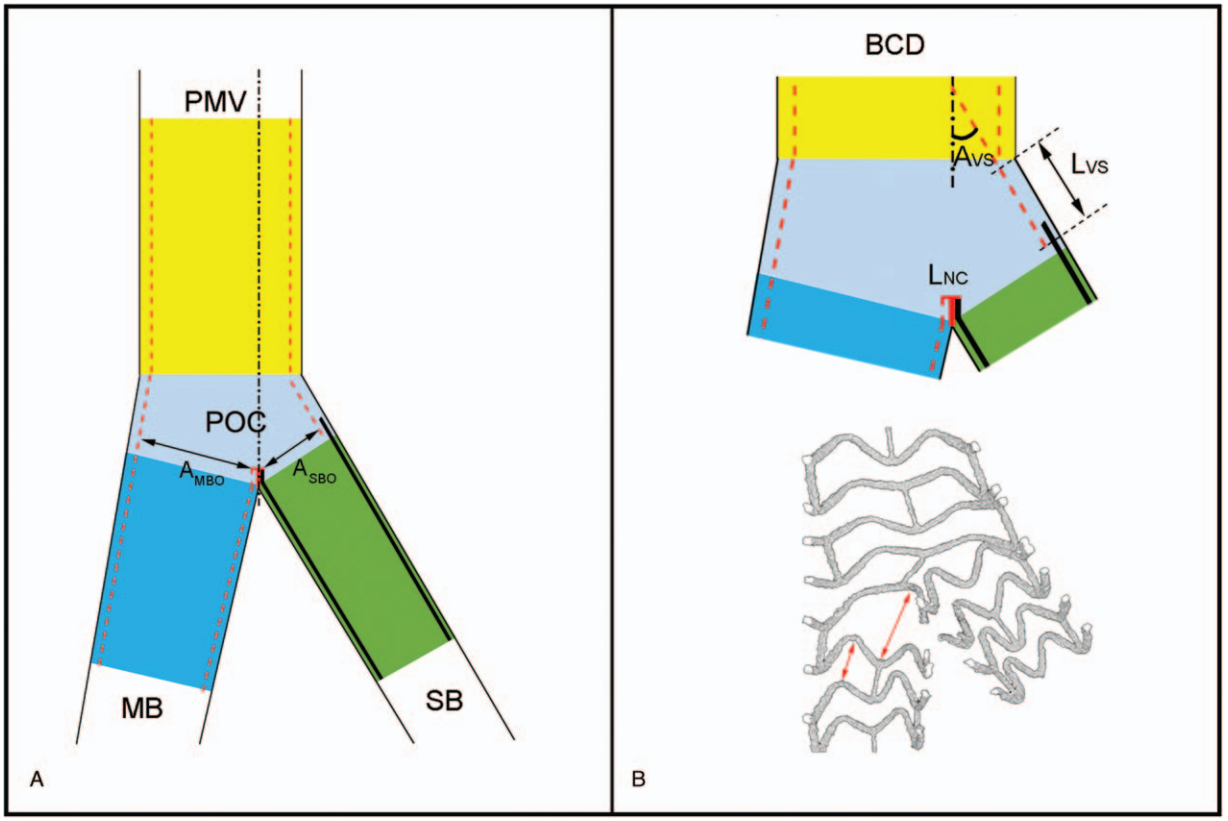

Figure 1. Bifurcation segmentation and scaffold morphological analysis. A, Schematic diagram of the bifurcated segmentation: the parent main-vessel (PMV), polygon of confluence (POC), main-branch (MB), and side-branch (SB). The figure also shows measurement of the branch ostial area (A_{OST}) including the MB ostial area (A_{MBO}) and SB ostial area (A_{SBO}), the reference area of scaffold lumen (A_{REF}), the length of neocarina (L_{NC}), and the length (L_{VS}) and angle (A_{VS}) of valgus struts at each point measured. B, Schematic diagram (upper) and 3D reconstructed image (lower) of bifurcation connecting domain (BCD) that comprised POC and its adjacent segments of 3 mm proximal to POC, 3 mm distal to SB and MB ostium. Additionally, the method for axially measuring the ring-ring distance (red double arrow) is shown for further analysis of scaffold distortion in BCD (lower). 3D = three dimensional.

(A_{MBO}) or SB (A_{SBO}) ostium, and the minimal (D_{MIN}) and maximal (D_{MAX}) diameter at the most asymmetric site, which was usually located in the BCD[22–24] (Fig. 1A). Based on the measurements, the index of scaffold lumen symmetry (I_{SLS}) was calculated by D_{MIN}/D_{MAX}, and the percentage of residual in-scaffold stenosis (P_{RIS}) was calculated by $100 \times (A_{REF} - A_{MIN})/A_{REF}$. Here, A_{MIN} may be equal or similar to A_{MBO} or A_{SBO} in most bench testing situations.

Additionally, geometrical distortion of the scaffold struts was analyzed in BCD (Fig. 1B). The ring-to-ring distance (D_1) measured along the scaffold long-axis was normalized by the nominated ring-to-ring distance (D_0), giving the cell distortion index (D_1/D_0). The total number of cells (N_0) and the cells with $D_1/D_0 \geq 1.5$ (N_1) were counted in BCD. The index of scaffold cell distortion was calculated using $100 \times N_1/N_0$.

2.5. OCT image acquisition and analysis

In this study, 2-dimensional optical coherence tomography (OCT) was performed using the C7-XRTM OCT imaging system with Dragonfly Duo OCT catheter (St. Jude Medical, St. Paul, MN). Automatic pullbacks were performed at 20 mm/s and recorded at 100 frames per second. All images were analyzed by an independent observer using proprietary software. For comparison purposes, malapposition of scaffold struts was calculated in BCD, it was graded by the following criteria: full apposition (no malapposition), incomplete apposition (malapposition >0 μm), marked malapposition (malapposition >200 μm), floating struts (malapposition >500 μm). The rate of severe strut malapposition was expressed as a percentage of the strut footprint with malapposition >200 μm, as described previously.[25,26]

2.6. Hemodynamic analysis

The modified computational fluid dynamics technique (CFD) was used to assess hemodynamics in the bifurcated scaffold phantoms.[27–29] Briefly, the 3D geometry of the scaffolded bifurcation was established based on microCT-generated raw data rather than virtually simulated data. Bifurcation was then segmented using self-developed code and a commercial software package Solidworks 2015 (Dassault Systèmes SolidWorks Corp, Waltham, MA). The fluid domains were subsequently discretized by unstructured tetrahedral/hexahedral mixed cells. Finally, the Navier–Stokes equations for 3D steady flow with rigid wall were solved by commercial CFD code CFX (ANSYS Inc, Canonsburg, PA).

For hemodynamic simulation, blood was assumed to be a viscous incompressible Newtonian fluid with dynamic viscosity 3.5 cP and density 1.06 g/mL.[30] The arteries were presumed to be nonslip rigid walls, and flow velocity at the vessel inlet was presumed to be fixed at 0.5 m/s. The hemodynamic parameters, including the wall shear stress (WSS) and its distribution, the flow velocity, and its streamlines, were assessed in the bifurcated scaffold phantoms, in particular, focused on BCD.

2.7. Statistical analysis

All data analyses were conducted using statistical software packages (SPSS 22.0; SSPS, Chicago, IL). Continuous variables are expressed as mean ± standard deviation and categorical data as counts (%). The Student *t* test was used for comparison of continuous variables. $P < 0.05$ was considered statistically significant.

3. Results

The device and procedural success were recorded for all tests in both groups without rupture of scaffolds. Typical examples were shown in Fig. 2 for comparison of OOT versus non-OOT. Figure 3 and Appendix Video A, http://links.lww.com/MD/C580 and B, http://links.lww.com/MD/C581 show comparisons of OPT to TAP morphologically; Fig. 4 shows a comparison of OPT to TAP hemodynamically.

3.1. Bifurcated scaffold morphologies

The morphological measurements are listed in Table 1. OOT created longer L_{VS} than non-OOT (2.49 ± 0.27 vs 1.78 ± 0.33 mm, $P < .01$) and broader A_{VS} (55.00 ± 4.18 vs 46.20 ± 6.14°, $P < .05$). Meanwhile, compared with TAP, OPT significantly improved ostial MB morphologies via shorter L_{NC} (0.34 ± 0.10 vs 1.02 ± 0.26 mm, $P < .01$), larger A_{MBO} (9.46 ± 0.04 vs 8.34 ± 0.09 mm^2, $P < .01$), less P_{RIS} (1.02 ± 0.55 vs 13.07 ± 1.09%, $P < .01$), and higher I_{SLS} (0.91 ± 0.03 vs 0.74 ± 0.06, $P < .01$) irrespective of similar optimal scaffold expansion along the PMV, MB, and SB, and at SB ostium observed in both treatments. OPT also tended to reduce the severity of scaffold distortion in BCD. OCT was associated with much less scaffold malapposition in OPT than TAP, as indicated by lower R_{SMA} in BCD (1.94 ± 0.54 vs 13.20 ± 1.66%, $P < .01$).

3.2. Bifurcated scaffold hemodynamics

Hemodynamic measurements are listed in Table 2. OPT generated better hemodynamic results than TAP: smaller area (14.41 ± 4.51 vs 26.60 ± 5.02 mm^2, $P < .01$) with lower area percentage (4.68 ± 1.40 vs 8.88 ± 1.21%, $P < .01$) of low WSS (defined by < 0.4 Pa) on branch lateral walls and higher magnitude of mean WSS on the scaffold luminal surface (1.53 ± 0.12 vs 1.26 ± 0.04 Pa, $P < .01$).

Qualitative analysis showed more favorable flow patterns produced by OPT, as shown in Fig. 4. TAP was associated with significantly lower PMV/MB flow velocity than OPT. The blood flow was also disturbed by creating microturbulence that distributed the area near the neo-carina, particularly on its MB side, suggesting that the protrusion of SB scaffold into POC inherent to TAP is the principal cause of disturbed flow patterns.

4. Discussion

BVSs offers an opportunity but also poses a challenge for PCI of CBLs because BVSs differ from the conventional metal stent platforms in many ways, such as the thicker struts and more fragile structure of the currently available BVS (PLLA-BVS).[31] In this way, the previous stenting techniques and associated procedural steps developed for metal stent platforms should be re-examined until they can be safely used with BVS.

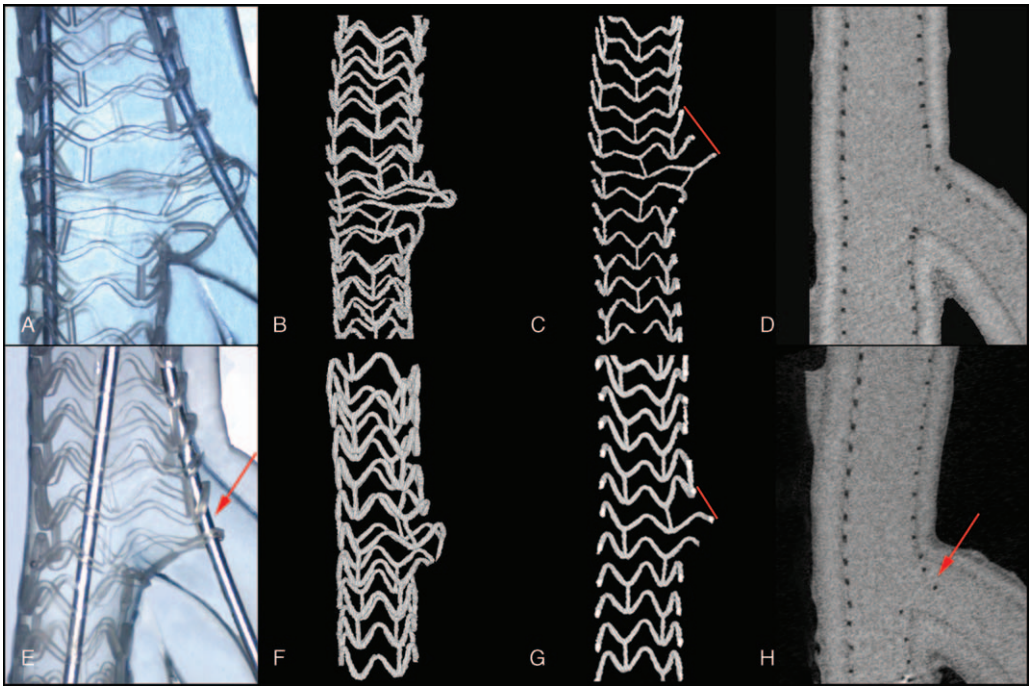

Figure 2. Morphological differences among SB ostia treated with OOT and non-OOT. Photos and microCT-reconstructed 3D images of bifurcated scaffolds showing OOT (upper panels A, B, C, D) to be more effective than non-OOT (lower panels E, F, G, H) with respect to overturning the redundant MB struts covering the SB ostium onto the superior border of ostial SB, resulting in ectropion in more struts, as shown in photos (A vs E, arrow), full 3D images (B vs F), and electronic haft-cut 3D images on the coronal plane (C vs G, solid line). In this particular case, ectropion of the struts could be created completely by OOT but only partially by non-OOT, as indicated by greater length and broader angle of the valgus strut in strut sectional images on the midline coronal plane (D vs H, arrow). 3D = three-dimensional, microCT = micro-computed tomography, OOT = ostial optimization technique, SB = side-branch.

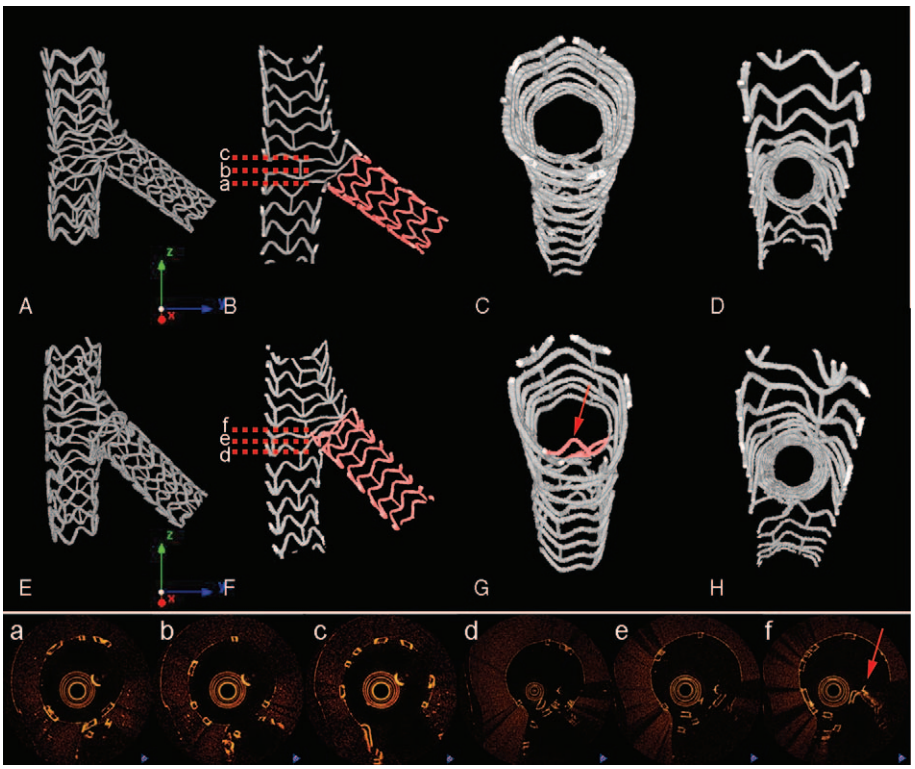

Figure 3. Morphological difference of bifurcated scaffold between OPT and TAP. MicroCT-reconstructed 3D images, electronic haft-cut 3D images, ostial MB, and SB images viewed from proximal side after electronic cutting of the full 3D images acquired for OPT (upper panels A, B, C, D) and TAP (middle panels E, F, G, H) showing OPT facilitate positioning of the SB scaffold due to better ectropion of the struts caused by OOT, thus resulting in a seamless connection and little overlap between the SB and MB scaffolds (A and B), while TAP required pulling the SB scaffold back into the PMV to completely cover the superior border of the ostial SB, thus resulting in longer neocarina (E and F vs A and B), smaller asymmetric MB ostium (G vs C, arrow), regardless of similar size and symmetry at their SB ostial in this case (D vs H). Additionally, OCT with imaging level at the carina, mid-POC, and proximal POC acquired for OPT (lower panels a, b, c) and TAP (lower panels d, e, f) showing that, compared with TAP, OPT was capable of achieving better strut apposition in BCD (a vs d, b vs e, c vs f), larger and more symmetric MB ostium (a vs d). BCD = bifurcation connecting domain, microCT = micro-computed tomography, OCT = optical coherence tomography, OPT = optimized provisional T-stenting, TAP = T-stenting and a small protrusion.

This is the first study to examine the feasibility of OOT in the optimization of the SB ostium and subsequent SB scaffolding. We also to compare the performance of OPT and TAP in bifurcation scaffolding with BVS. Our major findings were as follows: OOT overturn the redundant struts covering the SB ostium onto the superior border of the ostial SB without rupturing the MB scaffold, resulting in lip-like strut ectropion. OOT facilitated subsequent SB scaffold positioning and implantation without excessive protrusion of the rescue SB scaffold after T or T-stenting and small protrusion (TAP), resulting in seamless connection between the MB and SB scaffolds; OPT outperformed TAP in terms of bifurcated morphologies and hemodynamics.

4.1. Proper ways to accomplish OOT

Final single or kissing balloon dilation, once a standard step in enlargement of the side-hole of the MB stent in the treatment of CBLs with 1-stent approach was expected to optimize the SB ostium regardless of debate about its efficacy in reducing ostial SB restenosis or MACE.[32–35] Likewise, intermediate single or kissing balloon dilation was used to dilate the stent side-hole as well, mainly to facilitate subsequent stent passage when using CPT.[1,27,36–38] OOT differs from intermediate, final, single, and kissing balloon dilation in the following ways: it is a snuggling or mini-kissing balloon dilation technique rather than a standard technique; it was achieved by sequential intermediate snuggling balloon instead of routine intermediate balloon dilation, which were themselves achieved by first inflating the SB with higher pressure (10 atmospheres) followed by MB inflation of the noncompliant balloon at low pressure (6 atmospheres) for 30 seconds as using BVS; sequential intermediate snuggling balloon generated the resultant force better aligned to the natural SB axis, thereby producing better results, specifically a lip-like strut ectropion. In the present study, which was performed with BVS, OOT was associated with longer and more widely angled strut extropion than routine intermediate balloon dilation, resulting in 2-stent effects with 1-stent implantation and pronounced facilitation of subsequent SB scaffolding as the rescue SB stenting was indicated.

4.2. Differences in performance between OPT and TAP

Even though TAP simplifies the SB scaffold positioning process significantly with complete lesion coverage with respect to rescue SB stenting, stent over-protrusion into the PMV will alter bifurcated morphologies and hemodynamics,[28,34,39–41] which may become more severe with BVS due to its physical properties. OCT is accepted as a gold standard technique for the optimization of BVS implantation.[42] Due to its high resolution, OCT is useful to visualize and evaluate the scaffold struts in vivo. In addition, 3D OCT reconstruction is feasible to evaluate the ostium of SB jailed with BVS and guide selection of proper distal

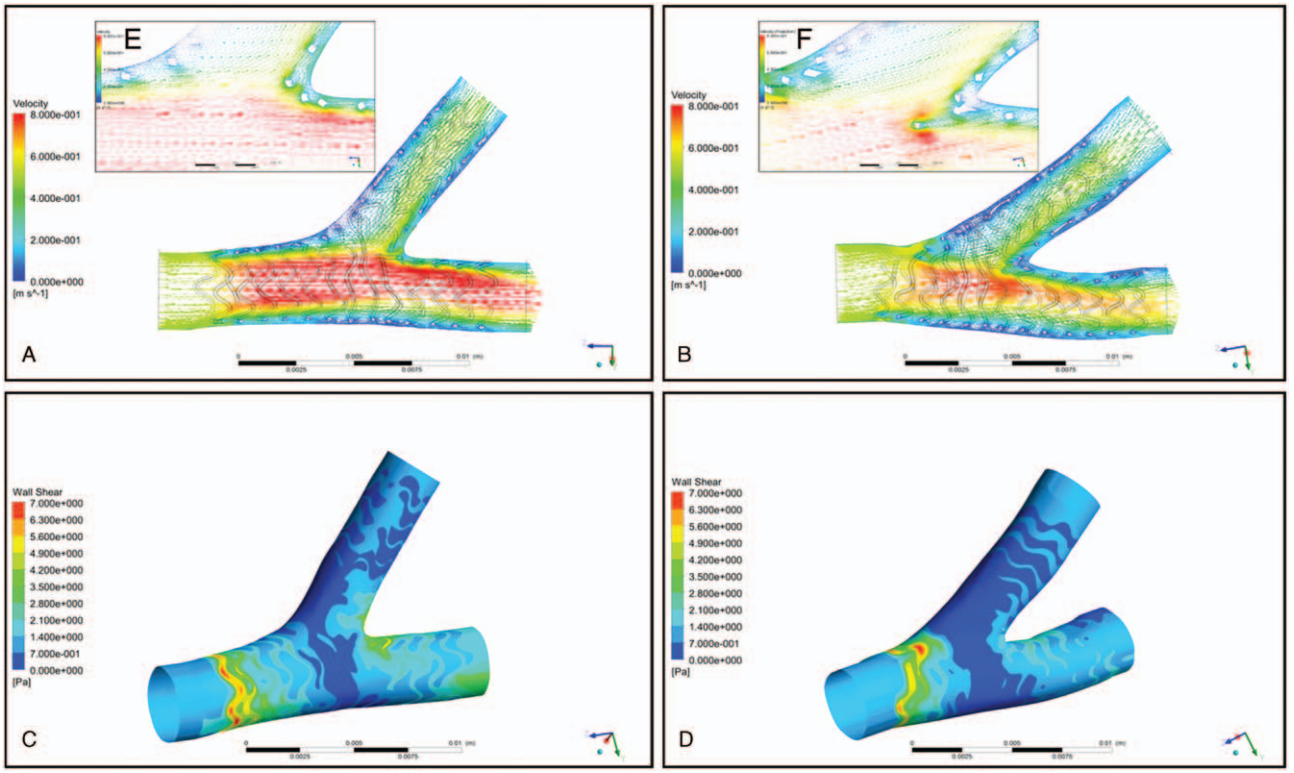

Figure 4. Hemodynamic difference of bifurcated scaffolds between OPT and TAP. Velocity streamlines, vorticity field, and wall shear stress distributions acquired with CFD based on microCT-reconstructed 3D images for OPT (left panels A, C) and TAP (right panels B, D). TAP was associated with significant abnormalities in flow pattern not observed in OPT, as evidenced by a decrease in flow velocity, particularly in the proximal MB opposite to the neo-carina, with locally disturbed stream lines and turbulent fields near the neo-carina (A vs B in zoomed pictures) and an increase in low shear stress area distributed mainly to the MB and SB lateral walls (C vs D). CFD = computational fluid dynamics technique, microCT = micro-computed tomography, OPT = optimized provisional T-stenting, TAP = T-stenting and a small protrusion.

cell for SB rewiring in provisional bifurcation stenting. Accordingly, systematic imaging assessment using OCT is essential to ensure optimal outcomes with BVS in clinical practice. CFD analysis is another invaluable method for the quantification of scaffold hemodynamics.[43] Previous studies have demonstrated that low WSS (<0.4 Pa) tends to be present in regions with erosion and plaques formation.[44,45] As shown in the present study, OPT was associated with much better bifurcated scaffold morphologies and hemodynamics than TAP, as clearly evidenced by the larger MB ostial area, shorter neocarina length, and greater luminal symmetry relative to microCT, less severe strut malopposition relative to OCT, smaller low WSS area on branches lateral walls, and less pronounced microturbulence near the neocarina by CFD.

4.3. Clinical relevance of OOT and OPT

Because BVS increases the risk of thrombosis, simpler approaches (1-scaffold or provisional T-stenting) remain the preferred treatments for most CBLs recommended by EBC consensus.[6–9] However, when using simpler approaches thicker scaffold across the ostial SB may more readily compromise the ostium, leading to acute occlusion and residual stenosis or to chronic strut occupation and restenosis.[46–49] There is no consensus on the treatment of struts crossing over the SB ostium. Single balloon or mini-kissing/snuggling balloon dilation has been suggested as more cautious means of expanding the scaffold side-hole at low pressure, but they cannot completely avoid destroying the scaffold structure. OOT with the unique sequential intermediate snuggling balloon technique could prevent distortion or rupture of the struts. More importantly, it creates a lip-like strut ectropion to cover the upper rim of the ostial SB, resulting in 2-scaffold effects with 1-scaffold implantation or avoidance of rescue SB stenting. Moreover, if rescue SB stenting is required, such as in cases of severely compromised SB, dissection, flow impairment, or any combination of these, OPT can easily produce a seamless connection between the SB and MB scaffolds, thereby reducing the risks of scaffold thrombosis.

BVS are considered the fourth revolution in the field of interventional cardiology and are emerging as a promising treatment for patients undergoing primary PCI. However, scrupulous lesion selection, appropriate implantation technique, and the application for systematic intravascular imaging assessment are crucial to achieving better long-term clinical outcome with the currently available devices.[50] For complex CBLs, as 2-scaffold strategy is indicated, only T-stenting is recommended by EBC consensus with avoiding complex techniques such as crush or culotte. However, classical T-scaffolding may bring in the issue of leaving an uncovered gap in ostial SB. This issue can be addressed with post-treatment of final sequential intermediate snuggling balloon (OOT) which, meanwhile, can effectively decrease the need of rescue SB scaffold.

4.4. Study limitations

Despite controlling the procedural cofounders that may affect the results, there are some limitations in our study. First, the model represents an idealized bifurcation without lesions, whereas CBLs

Table 1

Morphological comparison between OPT and TAP.

Variables	OPT (n=5)	TAP (n=5)	P
MCT analysis			
Along PMV			
A_{REF}, mm^2	10.22±0.05	10.23±0.03	.77
A_{MIN}, mm^2	10.12±0.05	10.15±0.04	.31
I_{SLS}	0.93±0.04	0.94±0.05	.78
P_{RIS}, %	1.05±0.32	0. 80±0.27	.22
Along MB			
A_{REF}, mm^2	9.45±0.02	9.44±0.03	.39
A_{MIN}, mm^2	9.28±0.05	9.25±0.05	.39
I_{SLS}	0.91±0.04	0.90±0.03	.82
$P_{RIS,\ \%}$	1.86±0.39	2.00±0.32	.54
At MB ostium			
$A_{MBO,}$ mm^2	9.46±0.04	8.34±0.09	<.01
I_{SLS}	0.91±0.03	0.74±0.06	<.01
$P_{RIS,}$ %	1.02±0.55	13.07±1.09	<.01
Along SB			
A_{REF}, mm^2	7.32±0.02	7.30±0.02	.15
A_{MIN}, mm^2	7.24±0.02	7.22±0.02	.17
I_{SLS}	0.94±0.01	0.91±0.03	.09
P_{RIS}, %)	1.10±0.52	1.12±0.35	.95
At SB ostium			
A_{SBO}, mm^2	7.31±0.03	7.29±0.02	.38
I_{SLS}	0.94±0.02	0.92±0.02	.14
P_{RIS} , %	3.12±0.76	3.16±0.32	.92
In BCD			
L_{VS} , mm	2.49±0.27	1.78±0.33	<.01
A_{VS} , °	55.00±4.18	46.20±6.14	<.05
L_{NC} , mm	0.34±0.10	1.02±0.26	<.01
I_{SLS}	0.50±0.07	0.49±0.08	.92
I_{SCD} , %	6.00±2.23	8.60±2.07	.09
OCT analysis			
R_{SMA}, BCD, %	1.94±0.54	13.20±1.66	<.01

Data are expressed as mean±SD.

A_{MBO}=area of MB ostium, A_{MIN}=minimal area of scaffold lumen, A_{REF}=reference area of scaffold lumen, A_{SBO}=area of SB ostium, A_{VS}=angle of valgus struts, BCD=bifurcation connecting domain, I_{SCD}=index of scaffold cell distortion, I_{SLS}=index of scaffold lumen symmetry, L_{NC}=length of neo-carina, L_{VS}=length of valgus struts, MB=main-branch, MCT=microcomputed tomography, OCT=optical coherence tomography, OPT=optimized provisional T-stenting, PMV=parent main-vessel, POC=polygon of confluence, P_{RIS}=percentage of residual in-scaffold stenosis, R_{SMA}=rate of severe strut mal-apposition, SB=side-branch, TAP=T-stenting and a small protrusion.

in real clinical settings are usually much more complicated, and the resultant scaffold morphology may be affected by the specific characteristics of the lesion or the patient's anatomy. Second, current CFD simulation was based on a steady flow model; while pulsatile flow might form more complex flow patterns. Third, the arteries were assumed to be non-slip rigid walls and the fluid properties to be typical coronary circulatory conditions for CFD simulations, which may not really reflect the clinical scenarios. Thus, further studies are warranted to confirm our observations.

Table 2

Hemodynamic comparison between OPT and TAP.

Variables	OPT (n=5)	TAP (n=5)	P
Total vascular wall area, mm^2	306.95±31.00	299.67±40.89	.76
Vascular wall area with low shear stress, <0.4 Pa, mm^2	14.41±4.51	26.60±5.02	<.01
Percent of wall area with low shear stress, <0.4 Pa, %	4.68±1.40	8.88±1.21	<.01
Mean scaffold wall shear stress, Pa	1.53±0.12	1.26±0.04	<.01

Data are expressed as mean±SD.

OPT=optimized provisional T-stenting, TAP=T-stenting and a small protrusion.

5. Conclusions

In conclusion, when using polymeric BVSs for treatment of CBLs, OOT is technically feasible for optimizing the SB ostium and facilitating the implantation of subsequent SB scaffolding; as required rescue SB scaffolding, OPT is associated with better bifurcated morphologies and hemodynamics than TAP, and such benefits may translate into improved clinical outcomes but further clinical validation is necessary.

Author contributions

Data curation: Linlin Zhang, Yukun Luo, Xingchun Zheng.
Formal analysis: Linlin Zhang, Xingchun Zheng.
Funding acquisition: Lianglong Chen.
Investigation: Sheng Tu, Zhaoyang Chen.
Methodology: Wei Cai, Sheng Tu, Lin Fan, Yukun Luo.
Project administration: Lin Fan.
Software: Zhaoyang Chen.
Supervision: Lianglong Chen.
Writing – original draft: Wei Cai.
Writing – review & editing: Lianglong Chen.
Wei Cai orcid: 0000-0001-8122-9744.

References

[1] Hildick-Smith D, de Belder AJ, Cooter N, et al. Randomized trial of simple versus complex drug-eluting stenting for bifurcation lesions: the British Bifurcation Coronary Study: old, new, and evolving strategies. Circulation 2010;121:1235–43.
[2] Steigen TK, Maeng M, Wiseth R, et al. Randomized study on simple versus complex stenting of coronary artery bifurcation lesions: the Nordic bifurcation study. Circulation 2006;114:1955–61.
[3] Levine GN, Bates ER, Blankenship JC, et al. 2011 ACCF/AHA/SCAI Guideline for Percutaneous Coronary Intervention. A report of the American College of Cardiology Foundation/American Heart Association Task Force on Practice Guidelines and the Society for Cardiovascular Angiography and Interventions. J Am College Cardiol 2011;58: e44–122.
[4] Behan MW, Holm NR, Curzen NP, et al. Simple or complex stenting for bifurcation coronary lesions: a patient-level pooled-analysis of the Nordic Bifurcation Study and the British Bifurcation Coronary Study. Cir Cardiovasc Interv 2011;4:57–64.
[5] D'Ascenzo F, Iannaccone M, Giordana F, et al. Provisional vs. two-stent technique for unprotected left main coronary artery disease after ten years follow up: a propensity matched analysis. Int J Cardiol 2016;211:37–42.
[6] Tamburino C, Latib A, van Geuns RJ, et al. Contemporary practice and technical aspects in coronary intervention with bioresorbable scaffolds: a European perspective. EuroIntervention 2015;11:45–52.
[7] Latib A, Capodanno D, Lesiak M, et al. Lessons from the GHOST-EU registry. EuroIntervention 2015;11(suppl V):V170–4.
[8] Fox J, Hossainy S, Rapoza R, et al. Technology limitations of BRS in bifurcations. EuroIntervention 2015;11(suppl V):V155–8.
[9] Stankovic G, Lassen JF. When and how to use BRS in bifurcations? EuroIntervention 2015;11(suppl V):V185–7.
[10] Lassen JF, Holm NR, Banning A, et al. Percutaneous coronary intervention for coronary bifurcation disease: 11th consensus document from the European Bifurcation Club. EuroIntervention 2016;12:38–46.
[11] Naganuma T, Colombo A, Lesiak M, et al. Bioresorbable vascular scaffold use for coronary bifurcation lesions: a substudy from GHOST EU registry. Catheter Cardiovasc Interv 2017;89:47–56.
[12] Sotomi Y, Suwannasom P, Serruys PW, et al. Possible mechanical causes of scaffold thrombosis: insights from case reports with intracoronary imaging. EuroIntervention 2017;12:1747–56.
[13] Cassese S, Kastrati A. Bioresorbable vascular scaffold technology benefits from healthy skepticism. J Am Coll Cardiol 2016;67:932–5.

[14] Di Mario C, Caiazzo G. Biodegradable stents: the golden future of angioplasty? Lancet 2015;385:10–2.
[15] Finn AV, Virmani R. The clinical challenge of disappearing stents. Lancet 2016;387:510–2.
[16] Stefanini GG, Holmes DRJr. Drug-eluting coronary-artery stents. N Engl J Med 2013;368:254–65.
[17] Kraak RP, Hassell ME, Grundeken MJ, et al. Initial experience and clinical evaluation of the Absorb bioresorbable vascular scaffold (BVS) in real-world practice: the AMC Single Centre Real World PCI Registry. EuroIntervention 2015;10:1160–8.
[18] Farag M, Spinthakis N, Gorog DA, et al. Use of bioresorbable vascular scaffold: a meta-analysis of patients with coronary artery disease. Open Heart 2016;3:e000462.
[19] Han Y, Xu B, Fu G, et al. A randomized trial comparing the NeoVas sirolimus-eluting bioresorbable scaffold and metallic everolimus-eluting stents. JACC Cardiovasc Interv 2018;11:260–72.
[20] Cai W, Zheng X, Luo Y. Provisional T-stenting with or without branch ostial optimization techniques for treatment of true bifurcation lesions. J Fujian Mad Univ 2017;51:391–5.
[21] Tu S, Hu F, Cai W, et al. Visualizing polymeric bioresorbable scaffolds with three-dimensional image reconstruction using contrast-enhanced micro-computed tomography. Int J Cardiovasc Imaging 2017;33:731–7.
[22] Robinson NM, Balcon R, Layton CA, et al. Intravascular ultrasound assessment of culotte stent deployment for the treatment of stenoses at major coronary bifurcations. Int J Cardiovasc Intervent 2001;4:21–7.
[23] Grundeken MJ, Ishibashi Y, Ramcharitar S, et al. The need for dedicated bifurcation quantitative coronary angiography (QCA) software algorithms to evaluate bifurcation lesions. EuroIntervention 2015;11(suppl V):V44–49.
[24] Sakata K, Koo BK, Waseda K, et al. A Y-shaped bifurcation-dedicated stent for the treatment of de novo coronary bifurcation lesions: an IVUS analysis from the BRANCH trial. EuroIntervention 2015;10:e1–8.
[25] Brown AJ, McCormick LM, Braganza DM, et al. Expansion and malapposition characteristics after bioresorbable vascular scaffold implantation. Cathete Cardiovasc Interv 2014;84:37–45.
[26] G Toth G, Pyxaras S, Mortier P, et al. Single string technique for coronary bifurcation stenting: detailed technical evaluation and feasibility analysis. JACC Cardiovasc Interv 2015;8:949–59.
[27] Foin N, Torii R, Mortier P, et al. Kissing balloon or sequential dilation of the side branch and main vessel for provisional stenting of bifurcations: lessons from micro-computed tomography and computational simulations. JACC Cardiovasc Interv 2012;5:47–56.
[28] Antoniadis AP, Giannopoulos AA, Wentzel JJ, et al. Impact of local flow haemodynamics on atherosclerosis in coronary artery bifurcations. EuroIntervention 2015;11(suppl V):V18–22.
[29] Chiastra C, Morlacchi S, Gallo D, et al. Computational fluid dynamic simulations of image-based stented coronary bifurcation models. J R Soc Interface 2013;10:20130193.
[30] Katritsis DG, Theodorakakos A, Pantos I, et al. Flow patterns at stented coronary bifurcations: computational fluid dynamics analysis. Circ Cardiovasc Interv 2012;5:530–9.
[31] Ormiston J, Darremont O, Iwasaki K, et al. Lessons from the real bench: non-BRS. EuroIntervention 2015;11(suppl V):V27–30.
[32] Ormiston JA, Webber B, Ubod B, et al. Absorb everolimus-eluting bioresorbable scaffolds in coronary bifurcations: a bench study of deployment, side branch dilatation and post-dilatation strategies. EuroIntervention 2015;10:1169–77.
[33] Niemela M, Kervinen K, Erglis A, et al. Randomized comparison of final kissing balloon dilatation versus no final kissing balloon dilatation in patients with coronary bifurcation lesions treated with main vessel stenting: the Nordic-Baltic Bifurcation Study III. Circulation 2011;123:79–86.
[34] Gutierrez-Chico JL, Gijsen F, Regar E, et al. Differences in neointimal thickness between the adluminal and the abluminal sides of malapposed and side-branch struts in a polylactide bioresorbable scaffold: evidence in vivo about the abluminal healing process. JACC Cardiovasc Interv 2012;5:428–35.
[35] Colombo A, Bramucci E, Sacca S, et al. Randomized study of the crush technique versus provisional side-branch stenting in true coronary bifurcations: the CACTUS (Coronary Bifurcations: Application of the Crushing Technique Using Sirolimus-Eluting Stents) Study. Circulation 2009;119:71–8.
[36] Burzotta F, Gwon HC, Hahn JY, et al. Modified T-stenting with intentional protrusion of the side-branch stent within the main vessel stent to ensure ostial coverage and facilitate final kissing balloon: the T-stenting and small protrusion technique (TAP-stenting). Report of bench testing and first clinical Italian-Korean two-centre experience. Catheter Cardiovasc Interv 2007;70:75–82.
[37] Kolpakov V, Polishchuk R, Bannykh S, et al. Atherosclerosis-prone branch regions in human aorta: microarchitecture and cell composition of intima. Atherosclerosis 1996;122:173–89.
[38] Finet G, Derimay F, Motreff P, et al. Comparative analysis of sequential proximal optimizing technique versus kissing balloon inflation technique in provisional bifurcation stenting: fractal coronary bifurcation bench test. JACC Cardiovasc Interv 2015;8:1308–17.
[39] Karanasos A, Li Y, Tu S, et al. Is it safe to implant bioresorbable scaffolds in ostial side-branch lesions? Impact of 'neo-carina' formation on main-branch flow pattern. Longitudinal clinical observations. Atherosclerosis 2015;238:22–5.
[40] Foin N, Alegria-Barrero E, Torii R, et al. Crush, Culotte, T and protrusion: which 2-stent technique for treatment of true bifurcation lesions? Circ J 2013;77:73–80.
[41] Migliavacca F, Chiastra C, Chatzizisis YS, et al. Virtual bench testing to study coronary bifurcation stenting. EuroIntervention 2015;11(suppl V): V31–34.
[42] Okamura T, Onuma Y, Garcia-Garcia HM, et al. 3-Dimensional optical coherence tomography assessment of jailed side branches by bioresorbable vascular scaffolds: a proposal for classification. JACC Cardiovasc Interv 2010;3:836–44.
[43] Caiazzo G, Longo G, Giavarini A, et al. Optical coherence tomography guidance for percutaneous coronary intervention with bioresorbable scaffolds. Int J Cardiol 2016;221:352–8.
[44] Malek AM, Alper SL, Izumo S. Hemodynamic shear stress and its role in atherosclerosis. JAMA 1999;282:2035–42.
[45] Campbell IC, Timmins LH, Giddens DP, et al. Computational fluid dynamics simulations of hemodynamics in plaque erosion. Cardiovasc Eng Technol 2013;4:464–73.
[46] Kawamoto H, Ruparelia N, Tanaka A, et al. Bioresorbable scaffolds for the management of coronary bifurcation lesions. JACC Cardiovasc Interv 2016;9:989–1000.
[47] Gori T, Schulz E, Hink U, et al. Early outcome after implantation of Absorb bioresorbable drug-eluting scaffolds in patients with acute coronary syndromes. EuroIntervention 2014;9:1036–41.
[48] Murata M, Matsubara Y, Kawano K, et al. Coronary artery disease and polymorphisms in a receptor mediating shear stress-dependent platelet activation. Circulation 1997;96:3281–6.
[49] Kawamoto H, Jabbour RJ, Tanaka A, et al. The bioresorbable scaffold: will oversizing affect outcomes? JACC Cardiovasc interv 2016;9:299–300.
[50] Indolfi C, De Rosa S, Colombo A. Bioresorbable vascular scaffolds—basic concepts and clinical outcome. Nature reviews. Cardiology 2016;13:719–29.